BLOCK DIFFERENTIAL ENCODING FOR RAPIDLY FADING CHANNELS

Bing Lu, Xiaoli Ma, and Georgios B. Giannakis

Dept. of ECE, University of Minnesota, Minneapolis, MN 55455, USA

ABSTRACT

Rapidly fading channels provide Doppler-induced diversity, but are also challenging to estimate. To by-pass channel estimation, we derive a novel block differential codec. Relying on a basis expansion model for time-varying channels, our block differential design is easy to implement, and achieves the maximum possible Doppler diversity. Simulation results corroborate our theoretical analysis.

1. INTRODUCTION

Modeling channel variations and coping with time-selective fading are important and challenging tasks in mobile communications. Pilot symbol assisted modulation (PSAM) offers an effective means of estimating time-selective channels with bandlimited variations [2], but is not designed to capitalize fully on Doppler diversity. As an alternative to PSAM, we develop in this paper a block differential scheme that obviates channel estimation, while enabling full diversity gains. Scalar differential phase shift keying (DPSK) has well documented merits; see also [3, 7] for recent results on improving the decoder's performance. Since diversity is known to combat fading, differential schemes have been designed to collect space-diversity [4, 5], and multipath diversity over frequency-selective channels using orthogonal frequency division multiplexing [1]. Existing differential schemes for time-selective channels, employ either multiple symbol detection (MSD) [3, 8], or, decision-feedback differential detection (DF-DD) [7, 8].

However, these approaches for time varying channels are not designed to exploit Doppler diversity gains, and may entail high decoding complexity. Based on an existing basis expansion model (BEM) [9], a block differential (BD) design is derived here, which applies block differential modualtion along with DF-DD, or, Viterbi decoding.

Notation: Upper (lower) bold face letters will be used for matrices (column vectors). Superscript $^{\mathcal{H}}$ will denote Hermitian, and ^{T} transpose. We will reserve E$[\cdot]$ for expectation, $\|\cdot\|$ for Frobenius norm. We will use $[\mathbf{A}]_{k,m}$ to denote the (k,m)th entry of a matrix $\mathbf{A}$, and $[\mathbf{x}]_m$ to denote the mth entry of the column vector $\mathbf{x}$; $\mathbf{I}_N$ will denote the $N \times N$ identity matrix, $\mathbf{1}_N$ an $N \times 1$ column vector of all-one entries; diag$[\mathbf{x}]$ will stand for a diagonal matrix with $\mathbf{x}$ on its main diagonal.

Work in this paper was supported by the ARL/CTA Grant No. DAAD19-01-2-011.

2. SYSTEM MODEL

Although extensions to multi-antenna systems are possible, in this paper we focus on single-antenna block transmissions over time-varying channels. The information bearing symbols $s(n)$ are drawn from a finite alphabet $\mathcal{A}_s$ with cardinality 2^R, where R denotes the transmission rate. They are parsed into blocks of size $N \times 1$: $[\mathbf{s}(k)]_n := s(kN + n - 1)$. Each information block $\mathbf{s}(k)$ is encoded by a differential encoder $\mathcal{D}(\cdot)$, whose output is (see also Fig. 1): $\mathbf{u}(k) := \mathcal{D}(\mathbf{s}(k))$. Since in the following we will work on a block-by-block basis, we will drop the block index k. Each block $\mathbf{u}$ is interleaved by a block interleaver $\mathbf{\Pi}$ with depth M. We take N to be an integer multiple of M. Later, we will show the relationship between M and N. Define the output of the interleaver $\mathbf{\Pi}$ as $\bar{\boldsymbol{u}} := \mathbf{\Pi}\mathbf{u}$. After parallel-to-serial (P/S) conversion, pulse shaping, and carrier modulation, the block $\bar{\boldsymbol{u}}$ is transmitted through a time-varying channel, whose delay spread is smaller than the symbol period T_s; hence, no frequency selectivity appears.

The nth sample at the receive-filter output (sampled with period equal to the symbol period T_s) is:

$$x(n) = \sqrt{\rho}\, h(n)\, \bar{u}(n) + w(n), \tag{1}$$

where ρ is the signal power per symbol, $h(n)$ is the aggregate time-selective impulse response that includes transmit-receive filters at the nth time slot, and $w(n)$ is additive white Gaussian noise (AWGN) with mean zero, and variance $N_0/2$. For the Doppler power spectrum of a mobile radio channel, the Jakes' model has been widely used [6]. As the number of parameters in the Jakes' model can be prohibitively large, we are motivated to consider the parsimonious BEM [9]. In its discrete-time baseband equivalent form, the BEM describes $h(n)$ as:

$$h(n) := \sum_{q=0}^{Q} h_q e^{j\omega_q n}, \tag{2}$$

where $\omega_q := 2\pi(q - Q/2)/N$, and $Q := 2\lceil f_{\max} N T_s \rceil$, with the parameter $f_{\max}$ denoting the maximum Doppler shift.

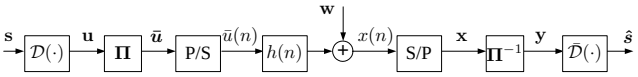

Fig. 1. Discrete-time block model of transmit-receiver.

Because it can be measured experimentally in practice, we assume that $f_{\max}$, and thus Q, are known and bounded (N and T_s are up to the designer's disposal). Time variation in the BEM (2) is captured by the discrete-time complex exponentials, while the coefficients $\{h_q\}_{q=0}^{Q}$ remain invariant over each block containing N symbols. A fresh set of BEM coefficients is considered every NT_s seconds.

At the receiver, the samples $x(n)$ are serial-to-parallel (S/P) converted to form the $N \times 1$ blocks with polyphase components $[\mathbf{x}]_i := x(i), i \in [0, N-1]$. The matrix-vector counterpart of (1) can then be expressed as:

$$\mathbf{x} = \sqrt{\rho}\, \mathbf{D}_h \bar{\boldsymbol{u}} + \mathbf{w}, \tag{3}$$

where $\mathbf{D}_h := \text{diag}[h(0), \ldots, h(N-1)]$, and $\mathbf{w}$ is defined similar to $\mathbf{x}$. Defining $[\mathbf{\Omega}]_{p+1,q+1} := \exp(j\omega_q p)$, and $[\mathbf{h}]_{q+1} := h_q,\ p \in [0, N-1], q \in [0, Q]$, we can express $\mathbf{D}_h$ as

$$\mathbf{D}_h = \text{diag}[\mathbf{\Omega h}]. \tag{4}$$

Each block $\mathbf{x}$ is deinterleaved by $\mathbf{\Pi}^{-1}$, to obtain $\mathbf{y} := \mathbf{\Pi}^{-1}\mathbf{x}$. Given the number of bases Q, we select $N = M(Q+1)$. Recalling that M is the depth of the interleaver, we obtain that interleaving and de-interleaving result in dividing the $N \times (Q+1)$ Vandermonde matrix $\mathbf{\Omega}$ into M non-overlapping sub-matrices $\{\mathbf{\Omega}_m\}_{m=0}^{M-1}$. Each sub-matrix $\mathbf{\Omega}_m$ is also a $(Q+1) \times (Q+1)$ Vandermonde matrix with $(k+1, q+1)$st entry $[\mathbf{\Omega}_m]_{k+1,q+1} = \exp[j\omega_q(m+kM)]$. Since $\mathbf{\Omega}_m^{\mathcal{H}}\mathbf{\Omega}_m = (Q+1)\mathbf{I}_{Q+1}$, it follows that $\mathbf{\Omega}_m$ is unitary. The equivalent channel matrix becomes

$$\mathbf{\Pi}^{-1}\mathbf{D}_h\mathbf{\Pi} = \text{diag}[\mathbf{h}_0^T, \mathbf{h}_1^T, \ldots, \mathbf{h}_{M-1}^T], \tag{5}$$

where $\mathbf{h}_m := [h(m), h(m+M), \ldots, h(m+QM)]^T = \mathbf{\Omega}_m\mathbf{h}, \forall m \in [0, M-1]$.

Using $\bar{\mathbf{u}} = \mathbf{\Pi u}$ and inserting (5) into (3), we can write the input-output relationship in a per sub-block form as

$$\mathbf{y}_m = \sqrt{\rho}\, \mathbf{D}_{h_m}\mathbf{u}_m + \mathbf{w}_m, \quad m \in [0, M-1], \tag{6}$$

where $[\mathbf{y}_m]_{q+1} = y(mM+q)$, $[\mathbf{u}_m]_{q+1} = u(mM+q)$, and $\mathbf{w}_m$ is defined similar to $\mathbf{h}_m$. Although we will use the BEM to quantify the diversity, our design (and (6)) applies to any time-selective channel model.

The block $\mathbf{y}_m$ is finally decoded by a differential decoder $\bar{\mathcal{D}}(\cdot)$ to obtain an estimate of $\mathbf{s}_m$: $\hat{\mathbf{s}}_m := \bar{\mathcal{D}}(\mathbf{y}_m)$.

3. BLOCK DIFFERENTIAL DESIGN

In this section, we will show how to design the differential encoder $\mathcal{D}(\cdot)$, and decoder $\bar{\mathcal{D}}(\cdot)$. These along with block (de-)interleaving will allow us to bypass channel estimation, and achieve the maximum possible Doppler diversity provided by our time-selective channel.

The differential encoder starts by splitting the $N \times 1$ vector $\mathbf{s}$ to obtain polyphase sub-blocks $\{\mathbf{s}_m\}_{m=0}^{M-1}$ with $[\mathbf{s}_m]_{q+1} := s(m(Q+1)+q), q \in [0, Q]$. Mapping $\mathbf{s}_m$ to $\mathbf{V}_m$, and generating $\mathbf{u}_m$ by using the unitary differential modulation of [4, 5] between consecutive sub-blocks, we obtain

$$\mathbf{u}_m = \begin{cases} \mathbf{V}_m\mathbf{u}_{m-1} & \text{if } 1 \le m \le M-1 \\ \mathbf{1}_{Q+1} & \text{if } m = 0, \end{cases} \tag{7}$$

where the $(Q+1) \times (Q+1)$ diagonal matrix $\mathbf{V}_m \in \boldsymbol{\mathcal{V}}$ conveys the information. As we have mentioned, each entry of $\mathbf{s}_m$ is chosen from a finite alphabet with cardinality 2^R; therefore, we need to design $\boldsymbol{\mathcal{V}}$ with cardinality $|\boldsymbol{\mathcal{V}}| = 2^{R(Q+1)}$. A simple design comprises a commutative group $\boldsymbol{\mathcal{V}}$ of diagonal matrices with $2^{R(Q+1)}$ elements so as to make it cyclic, as in [4]; thus, $\mathbf{V}_m$ is unitary.

By interchanging $\mathbf{D}_{h_m}$ with $\mathbf{u}_m$ in (6), we have $\mathbf{D}_{h_m}\mathbf{u}_m = \mathbf{D}_{u_m}\mathbf{\Omega}_m\mathbf{h}$. Because the BEM coefficient vector $\mathbf{h}$ remains unchanged across sub-blocks of the same block, and $\mathbf{D}_{u_m}$, $\mathbf{\Omega}_m$ are unitary, considering two consecutive sub-blocks, we obtain [c.f. (6)]

$$\mathbf{y}_m = \mathbf{D}_{u_m}\boldsymbol{\Upsilon}\mathbf{D}_{u_{m-1}}^{\mathcal{H}}\mathbf{y}_{m-1} + \mathbf{w}'_m, \forall m \in [1, M-1], \tag{8}$$

where $\boldsymbol{\Upsilon} := \mathbf{\Omega}_m\mathbf{\Omega}_{m-1}^{\mathcal{H}}/(Q+1)$ is independent of m, and $\mathbf{w}'_m := \mathbf{w}_m - \mathbf{D}_{u_m}\boldsymbol{\Upsilon}\mathbf{D}_{u_{m-1}}^{\mathcal{H}}\mathbf{w}_{m-1}$ is AWGN because $\mathbf{D}_{u_m}\boldsymbol{\Upsilon}\mathbf{D}_{u_{m-1}}^{\mathcal{H}}$ is a unitary matrix. Because $\mathbf{w}_m$ and $\mathbf{w}_{m-1}$ are independent, the covariance matrix of $\mathbf{w}'_m$ is $N_0\mathbf{I}_{Q+1}$. Note that because $\boldsymbol{\mathcal{V}}$ is a cyclic group, $\mathbf{D}_{u_m} = \prod_{l=1}^{m}\mathbf{V}_l \in \boldsymbol{\mathcal{V}}$.

Based on (8), detecting $\mathbf{D}_{u_m}$ will depend not only on the received vectors $\mathbf{y}_m$ and $\mathbf{y}_{m-1}$, but also on the symbols transmitted in earlier intervals. This is because the equivalent channels vary across sub-blocks. To cope with the multi-symbol dependence in (8), we will develop two detectors: one utilizing block DF-DD, and the other relying on the Viterbi algorithm (VA).

Letting $\hat{\mathbf{D}}_{u_{m-1}}$ denote the estimate of $\mathbf{D}_{u_{m-1}}$, our block DF-DD is defined as

$$\hat{\mathbf{D}}_{u_m} = \arg\min_{\tilde{\boldsymbol{D}} \in \boldsymbol{\mathcal{V}}} \|\mathbf{y}_m - \tilde{\boldsymbol{D}}\boldsymbol{\Upsilon}\hat{\mathbf{D}}_{u_{m-1}}^{\mathcal{H}}\mathbf{y}_{m-1}\|. \tag{9}$$

To mitigate error propagation, one can resort to multi-symbol detection (MSD), which in our case detects multiple sub-blocks, but also increases decoding complexity exponentially. Instead, we recommend the VA which uses ML sequence detector as:

$$\{\hat{\mathbf{D}}_{u_m}\}_{m=1}^{M-1} = \arg\min_{\forall \tilde{\boldsymbol{D}}_{u_m} \in \boldsymbol{\mathcal{V}}} \sum_{m=1}^{M-1} \|\mathbf{y}_m - \tilde{\boldsymbol{D}}_{u_m}\boldsymbol{\Upsilon}\tilde{\boldsymbol{D}}_{u_{m-1}}^{\mathcal{H}}\mathbf{y}_{m-1}\|^2. \tag{10}$$

Because the decision on $\hat{\mathbf{D}}_{u_m}$ depends only on a single previous sub-block $\mathbf{D}_{u_{m-1}}$, we design a VA with $|\boldsymbol{\mathcal{V}}| = 2^{R(Q+1)}$ states at one stage. Using VA searching through a trellis with $M-1$ stages, we can estimate $\{\mathbf{D}_{u_m}\}_{m=1}^{M-1}$.

Based on either DF-DD or VA, we can obtain $\hat{\mathbf{V}}_m = \hat{\mathbf{D}}_{u_{m-1}}^{\mathcal{H}} \hat{\mathbf{D}}_{u_m}$. The estimate of $\mathbf{s}_m$ can be found by demapping $\hat{\mathbf{V}}_m$ to $\hat{\mathbf{s}}_m$. Notice that the block DF-DD has complexity of $\mathcal{O}(2^{R(Q+1)})$, while the VA has slightly higher complexity of $\mathcal{O}(2^{2R(Q+1)})$.

4. PERFORMANCE ANALYSIS

In Sections 2 and 3, we developed a block differential (BD) scheme for time-selective channels. In this section, we will show that our design guarantees maximum Doppler diversity at least for high SNR. Our derivations are based on the following operating conditions:

AS1) BEM coefficients $\{h_q\}_{q=0}^{Q}$ are zero-mean, complex Gaussian random variables;

AS2) High SNR is considered only for deriving the diversity order.

If we consider each sub-channel in $\mathbf{h}_m$ (5) as a transmit-antenna, our single-antenna setup can be viewed as a system with $Q+1$ transmit- and one receive-antennae, similar to that considered in e.g., [4]. Employing (8) at the receiver, we will analyze the pairwise error probability (PEP), $\Pr[\mathbf{V}_m \to \mathbf{V}'_m]$, that $\mathbf{V}_m$ is incorrectly decoded as $\mathbf{V}'_m \neq \mathbf{V}_m$ [4, 5]. Based on AS2), we ignore the noise term in (8). Plugging (7) into (8), and relating $\mathbf{y}_{m-1}$ to $\mathbf{h}$, we obtain the conditional PEP by using the Chernoff bound:

$$\Pr[\mathbf{V}_m \to \mathbf{V}'_m|\mathbf{h}] \leq \exp\left[-\frac{\|\sqrt{\rho}\,[\mathbf{V}'_m - \mathbf{V}_m]\mathbf{D}_{u_{m-1}}\boldsymbol{\Upsilon}\boldsymbol{\Omega}_{m-1}\mathbf{h}\|^2}{8N_0}\right] \quad (11)$$

It is worth mentioning that the variance of $\mathbf{w}'_m$ in (8) is N_0 which is twice that of $\mathbf{w}_m$, consistent with the well known 3dB loss in SNR that differential detectors exhibit relative to coherent ones.

Although the channel is unknown at the receiver, based on AS1), (11) allows us to average the conditional PEP over the Rayleigh distributed channel parameters. Defining $\mathbf{R}_h := E[\mathbf{h}\mathbf{h}^{\mathcal{H}}]$, and eigen-decomposing $\mathbf{R}_h$, we find $\mathbf{R}_h = \mathbf{U}_h\boldsymbol{\Lambda}_h\mathbf{U}_h^{\mathcal{H}}$, where $\boldsymbol{\Lambda}_h = \text{diag}[\lambda_0, \ldots, \lambda_{r_h-1}]$ contains the non-zero eigenvalues of $\mathbf{R}_h$, and r_h is the rank of $\mathbf{R}_h$. The average PEP $\Pr[\mathbf{V}_m \to \mathbf{V}'_m]$ depends on the rank of the matrix $\mathbf{A}_m := (\mathbf{V}_m - \mathbf{V}'_m)\mathbf{D}_{u_{m-1}}\boldsymbol{\Upsilon}\boldsymbol{\Omega}_{m-1}\mathbf{U}_h\boldsymbol{\Lambda}_h^{1/2}$. Thus, the maximum Doppler diversity is defined as

$$G_d = \min_{\forall \mathbf{V}_m \neq \mathbf{V}'_m} \text{rank}(\mathbf{A}_m). \quad (12)$$

If the correlation matrix $\mathbf{R}_h$ has full rank, i.e., $r_h = Q+1$, and no error propagation occurs, then the maximum diversity $Q+1$ is achieved by our differential scheme with $\boldsymbol{\mathcal{V}}$ designed as in [4, 5].

Note that in our BD scheme, we fix the sub-block length to $Q+1$. If the length of each sub-block is smaller than $Q+1$, then $\boldsymbol{\Omega}_m$ is not unitary; i.e., $\boldsymbol{\Omega}_m^{\mathcal{H}}\boldsymbol{\Omega}_m \neq (Q+1)\mathbf{I}_{Q+1}$, and the differential detectors in (9) and (10) are no longer applicable. When the sub-block size is greater than $Q+1$, the code design and decoding both become more complex, while the performance may not improve.

Since one sub-block is used to initialize the differential recursion (7), the bandwidth efficiency (defined as the ratio of the number of information-bearing symbols over the block size) is given by:

$$\eta := \frac{N-(Q+1)}{N} = 1 - \frac{Q+1}{N}. \quad (13)$$

Accounting for the pilot symbols per PSAM block (which is an alternative to coping with time-varying channels), the bandwidth efficiency is $\eta_{psam} = 1-(Q+1)/N$, which is identical to (13). Note that scalar DPSK affords bandwidth efficiency $\eta_{dpsk} = 1 - 1/N$, which is higher than (13).

5. SIMULATED PERFORMANCE

For all test cases QPSK modulation is selected, leading to a transmission rate $R=2$. The cardinality of $\boldsymbol{\mathcal{V}}$ is $2^{R(Q+1)}$ for different Qs. The signal-to-noise ratio (SNR) is defined as E_b/N_0, where E_b is the signal power per information bit.

Test case 1 (Error propagation effects and performance comparisons): The $Q+1$ BEM coefficients are generated as complex Gaussian distributed with zero-mean. We select $Q = 2, 4$ corresponding to $f_{\max}T_s = 0.02, 0.04$, and decide the block length as $N = 48, 50$, respectively. The bit-error-rate (BER) performance is plotted in Fig. 2. We notice that the error propagation effect on the performance of our DF-DD is small (less than 0.3 dB), or, even negligible. This is because the initial sub-block is known, and the decision of the current sub-block only depends on a single previous sub-block. In addition, Viterbi decoding is considered for $Q = 2$, and we can see that both DF-DD and Viterbi decoding provide almost identical boost in performance.

In this case, we also plot the benchmark performance of coherent receivers when $Q=2$, assuming that the channel is perfectly known at the receiver. Note that the "3 dB difference" complies with our analysis in Section 4. Relying on the BEM, we also compare here the BER performance of our differential design with PSAM [2]. From these curves, we observe that: i) as Q increases, the performance of our BD scheme improves, because faster varying channels introduce more Doppler diversity; whereas for PSAM, the diversity order is always about one, irrespective of Q; and ii) for medium to large SNR values, the performance gain in our design with $Q=4$ outperforms PSAM as much as 10 dB at BER$= 10^{-3}$.

Test case 2 (Performance comparison with [8]): The channel is generated based on the Jakes' model [6, p.68] with $f_{\max}T_s = 0.02$, and the block length is chosen to be $N = 100$. The BER performance is depicted in Fig. 3. Note that although our BD scheme is not designed based on Jakes' model, it still enjoys Doppler diversity gains. However, the scheme in [8] can only achieve diversity one. Compared with [8], the price we pay is longer decoding delays because of the block interleaver.

Test case 3 (Performance comparison with [3]): Select $N = 180$, and $f_{\max}T_s = 0.01$. Again, Jakes' model is used to generate the channels. We select the design in [3] as an MSD representative. Different MSD sizes ($N_{MSD} = 1, 3, 5$) are tested. Fig. 4 depicts the simulated performance. Thanks to the block differential design at the transmitter, our scheme achieves higher diversity than [3] with comparable decoding complexity when $N_{MSD} = 5$. The MSD in [3] though, exhibits diversity order one. However, our BD has relatively longer decoding delays, higher decoding complexity, and lower bandwidth efficiency.

6. REFERENCES

[1] K. L. Baum and N. S. Nadgauda, "A comparison of differential and coherent reception for a coded OFDM system in a low c/i environment," in *Proc. of GlobeCom*, pp. 300–304, Nov. 1997.

[2] J. K. Cavers, "Pilot symbol assisted modulation and differential detection in fading and delay spread," *IEEE Trans. on Commu.*, pp. 2206–2212, July 1995.

[3] P. Ho and D. Fung, "Error performance of multiple-symbol differential detection of PSK signals transmitted over correlated Rayleigh fading channels," *IEEE Trans. on Commu.*, pp. 1566–1569, Oct. 1992.

[4] B. Hochwald and W. Sweldens, "Differential unitary space-time modulation," *IEEE Trans. on Commu.*, pp. 2041–2052, Dec. 2000.

[5] B. L. Hughes, "Differential space-time modulation," *IEEE Trans. on IT*, pp. 2567–2578, Nov. 2000.

[6] W. C. Jakes, *Microwave Mobile Communications*, New York: Wiley, 1974.

[7] R. Schober, W. H. Gerstacker, and J. B. Huber, "Decision-feedback differential detection of M-DPSK for flat rayleigh fading channels," *IEEE Trans. on Commu.*, pp. 1025–1035, July 1999.

[8] R. Schober and L. H. J. Lampe, "Noncoherent receivers for differential space-time modulation," *IEEE Trans. on Commu.*, pp. 768–777, May 2002.

[9] M. K. Tsatsanis and G. B. Giannakis, "Equalization of rapidly fading channels: Self recovering methods," *IEEE Trans. on Commu.*, pp. 619–630, May 1996.

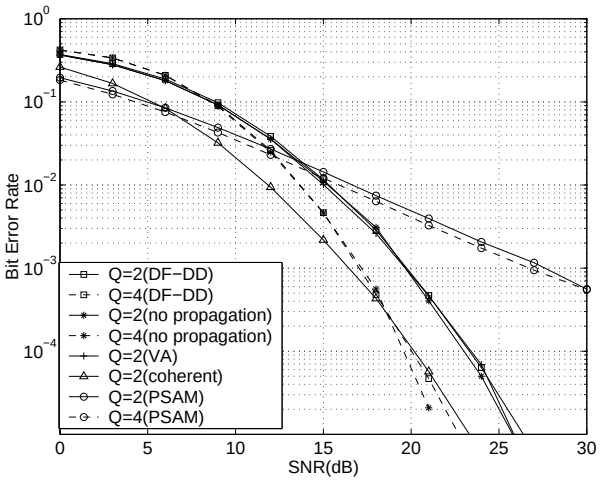

Fig. 2. Error propagation effects and performance comparisons with coherent receivers and PSAM

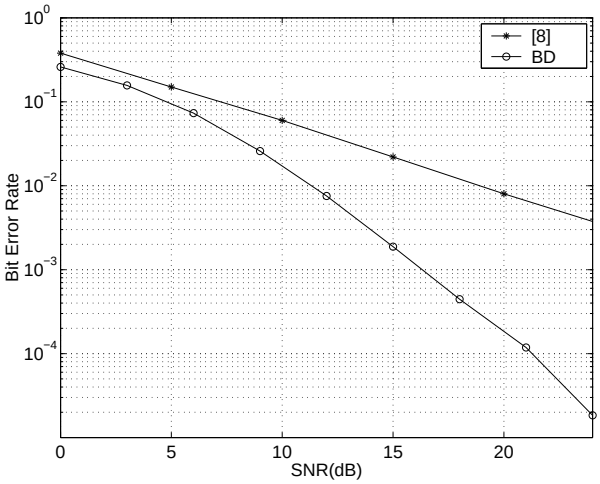

Fig. 3. Performance comparison of BD with [8]

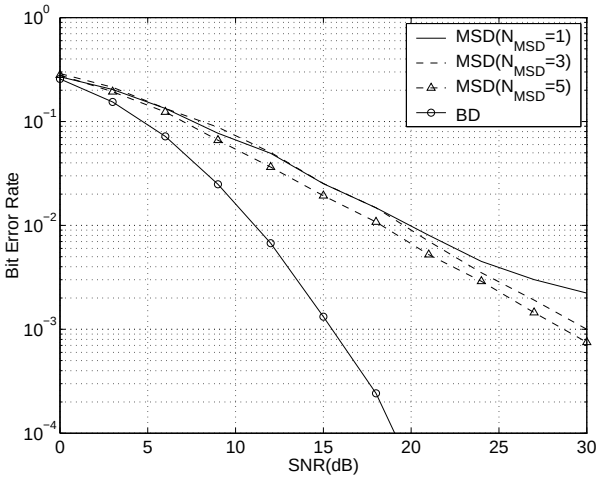

Fig. 4. Performance comparison of BD with [3]